

Supporting Information

Polymer non-fullerene solar cells of vastly different efficiencies for minor side-chain modification: Impact of charge transfer, carrier lifetime, morphology and mobility

Omar M. Awartani, Bhoj Gautam, Wenchao Zhao, Robert Younts, Jianhui Hou*, Kenan Gundogdu* and Harald Ade*

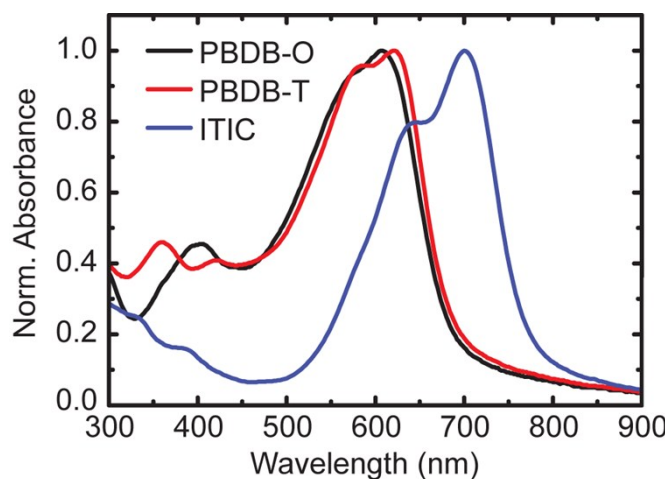


Figure S1. Normalized UV-Vis absorbance for PBDB-O, PBDB-T and ITIC neat films.

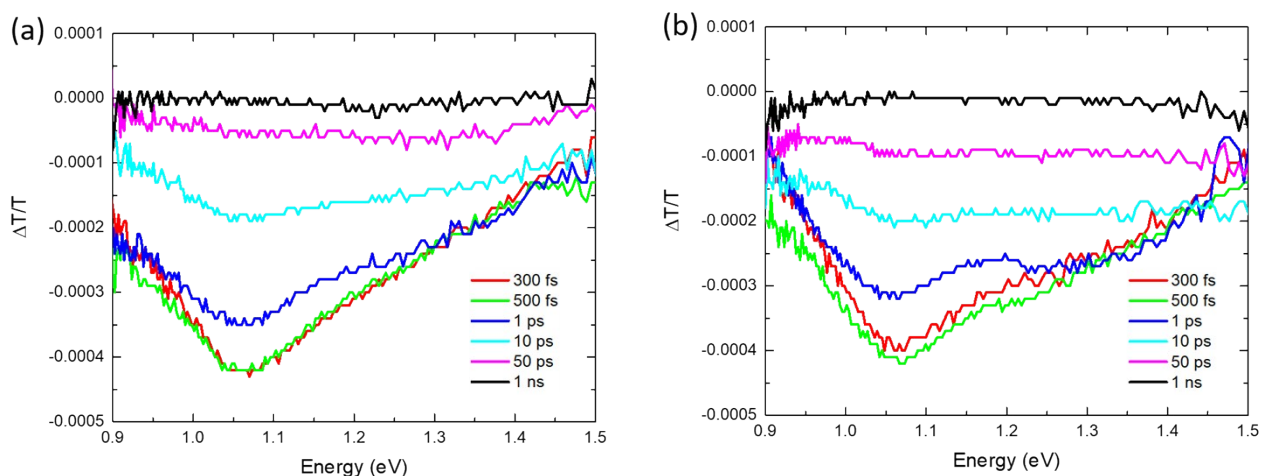


Figure S2: IR transient absorption spectra after an excitation at 520 nm (2.38 eV) probed at 0.3 ps, 0.5 ps, 1 ps, 10 ps, 50 ps and 1 ns delay times for neat a) PBDB-O, b) PBDB-T.

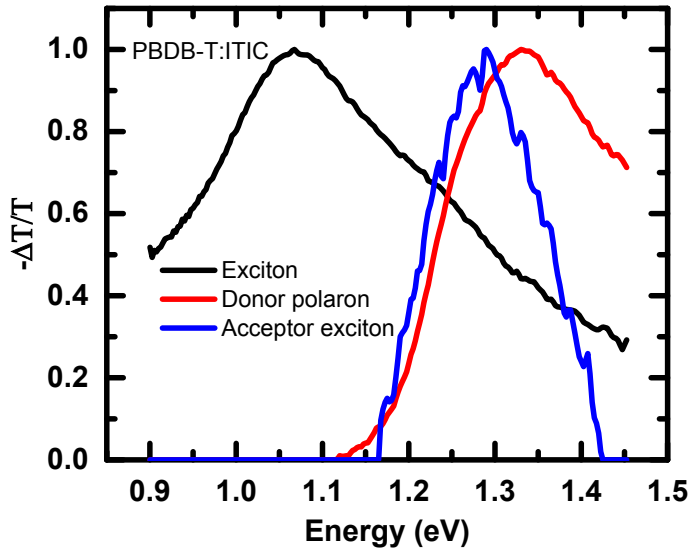


Figure S3: An example of deconvolution of the IR transient absorption spectra using MCR-ALS.

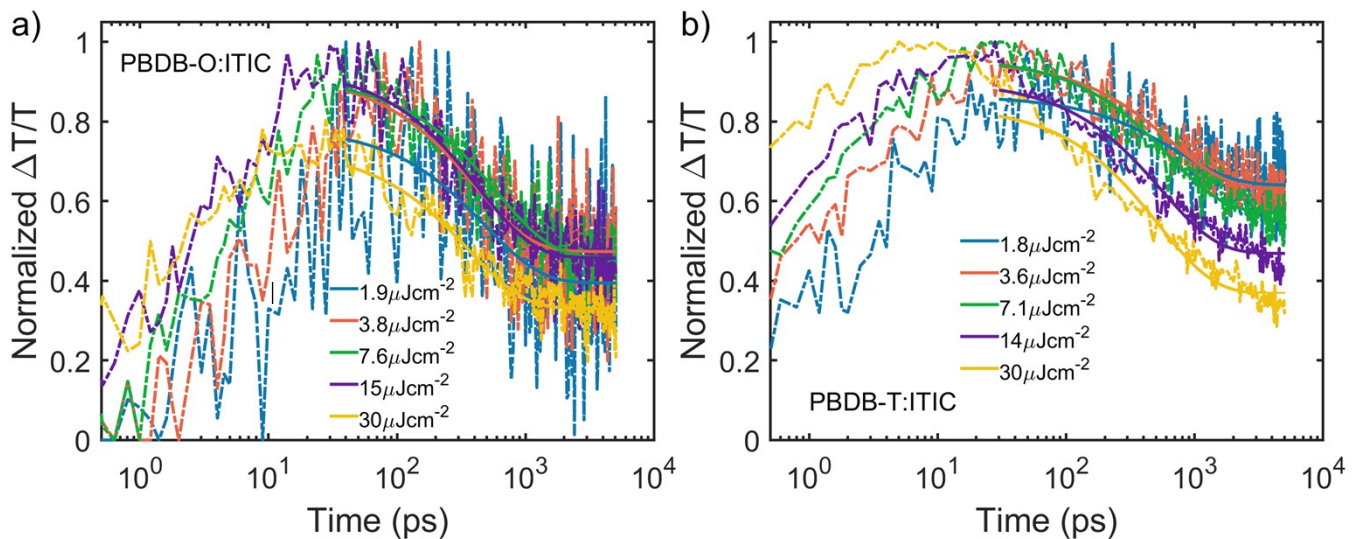


Figure S4: Normalized time evolution of polarons determined from MCR-ALS analysis for the donor excitation (2.28 eV) at the indicated fluences for a) PBDB-O:ITIC, b)PBDB-T:ITIC.

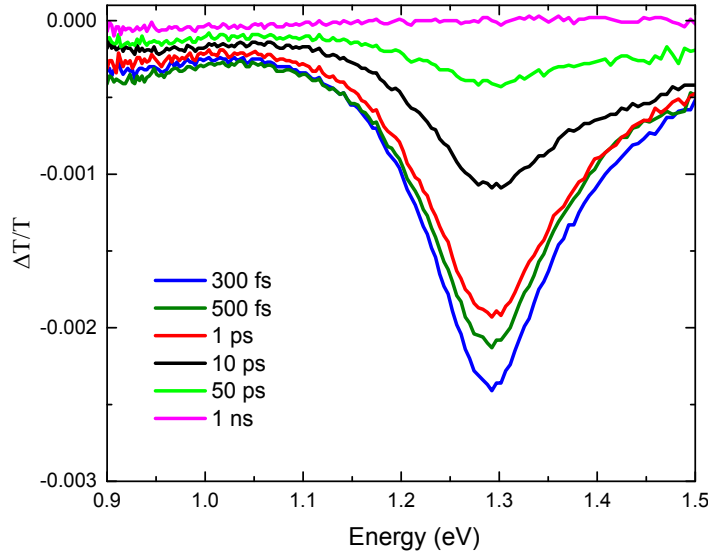


Figure S5: IR transient absorption spectra of neat ITIC after an excitation at 700 nm (1.77 eV) probed at 0.3 ps, 0.5 ps, 1 ps, 10 ps, 50 ps and 1 ns delay times.

Table S1: Fit parameters from exponential tail fits shown in Figure 3a and 3b for polaron dynamics of PBDB-O:ITIC and PBDB-T:ITIC blend films as a function of excitation fluence for the donor excitation of 2.38 eV.

Sample	Fluence ($\mu J \text{ cm}^{-2}$)	A_1 (%)	τ (ps)	A_2 (%)
PBDB-O:ITIC	1.88	50%	486 ± 150	50%
PBDB-O:ITIC	3.77	48%	407 ± 180	52%
PBDB-O:ITIC	7.55	50%	594 ± 64	50%
PBDB-O:ITIC	15.0	51%	429 ± 45	49%
PBDB-O:ITIC	30.1	55%	361 ± 32	45%
PBDB-T:ITIC	1.79	26%	750 ± 190	74%
PBDB-T:ITIC	3.57	34%	656 ± 61	66%
PBDB-T:ITIC	7.14	41%	624 ± 39	59%
PBDB-T:ITIC	14.28	48%	550 ± 29	52%
PBDB-T:ITIC	29.6	56%	522 ± 27	44%

Table S2: The percentage of ultrafast charge generation with 500 fs taken as the ratio of transient absorption signal from the polaron dynamics at 500 fs versus the maximum polaron signal.

Sample	Fluence ($\mu J \text{ cm}^{-2}$)	Peak Polaron TA Signal ($\times 10^{-3}$)	Percentage of Ultrafast Charge Generation (<500fs)
PBDB-O:ITIC	1.79	0.34 ± 0.05	$7 \pm 11\%$
PBDB-O:ITIC	3.57	0.71 ± 0.03	$7 \pm 11\%$
PBDB-O:ITIC	7.14	1.2 ± 0.07	$11 \pm 13\%$
PBDB-O:ITIC	14.28	1.9 ± 0.04	$29 \pm 11\%$
PBDB-O:ITIC	29.6	2.9 ± 0.03	$37 \pm 8\%$
PBDB-T:ITIC	1.88	0.11 ± 0.05	$35 \pm 10\%$
PBDB-T:ITIC	3.77	0.18 ± 0.04	$39 \pm 10\%$
PBDB-T:ITIC	7.55	0.39 ± 0.06	$47 \pm 8\%$

PBDB-T:ITIC	15.0	0.68 ± 0.08	$58 \pm 7\%$
PBDB-T:ITIC	30.1	1.1 ± 0.07	$76 \pm 4\%$

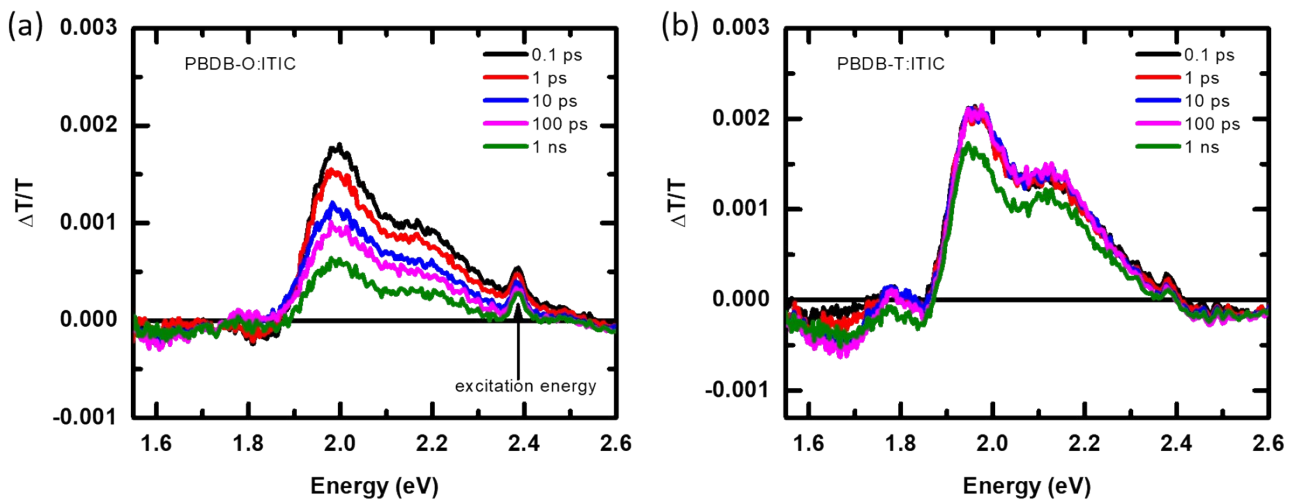


Figure S6: Visible range transient absorption spectra after an excitation at 520 nm (2.38 eV) probed at 0.3 ps, 0.5 ps, 1 ps, 10 ps, 100 ps and 1 ns delay times for a) PBDB-O:ITIC, b) PBDB-T:ITIC.

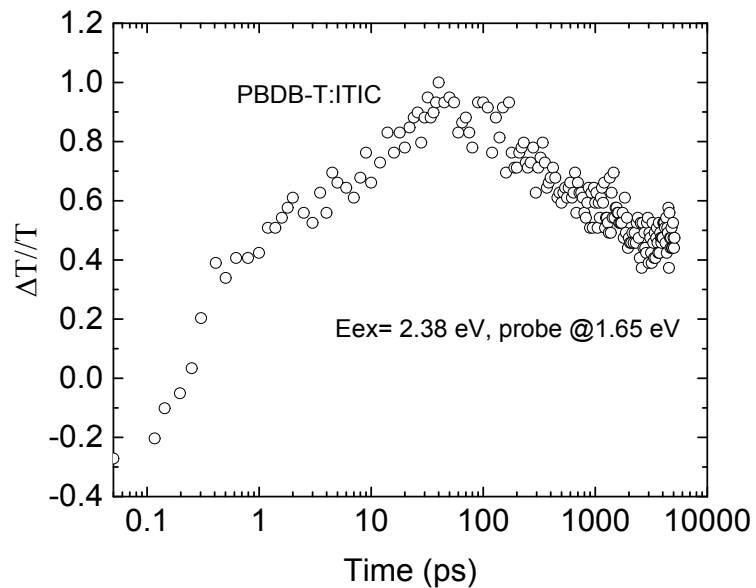


Figure S7: TA dynamics of PBDB-T:ITIC blend excited at 2.38 eV and probed at 1.65 eV.

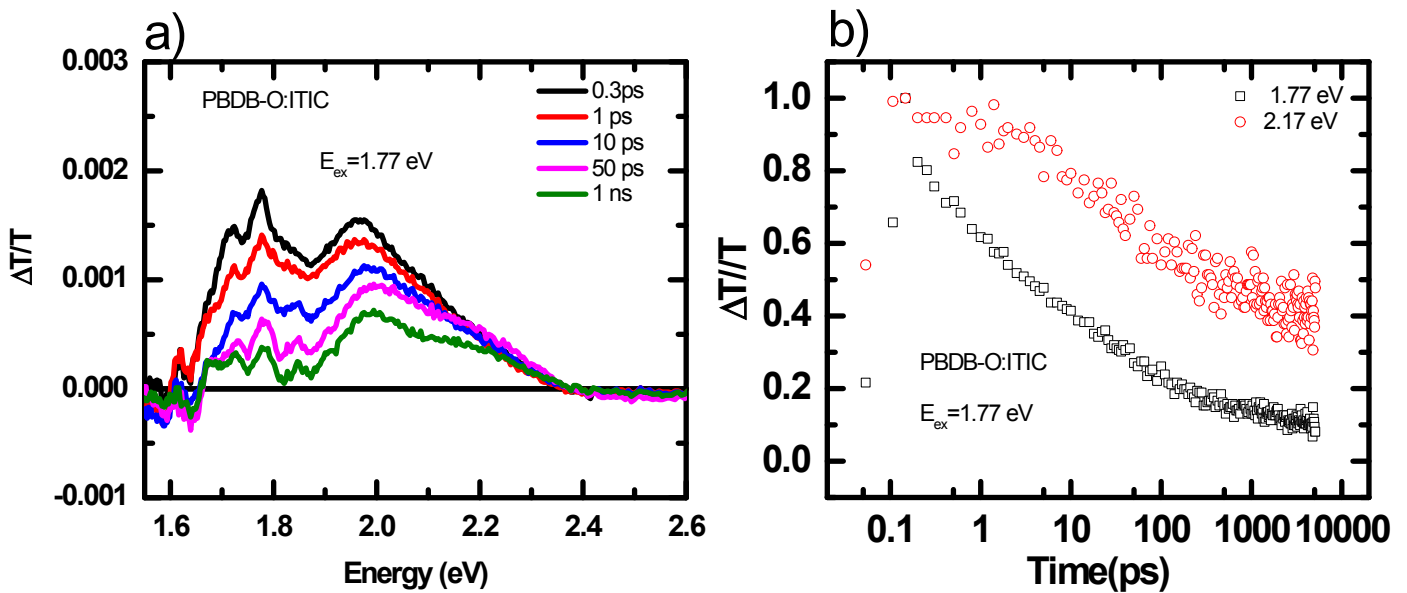


Figure S8: Visible range transient absorption spectra and transient absorption dynamics of PBDB-O:ITIC with 1.77 eV excitation.

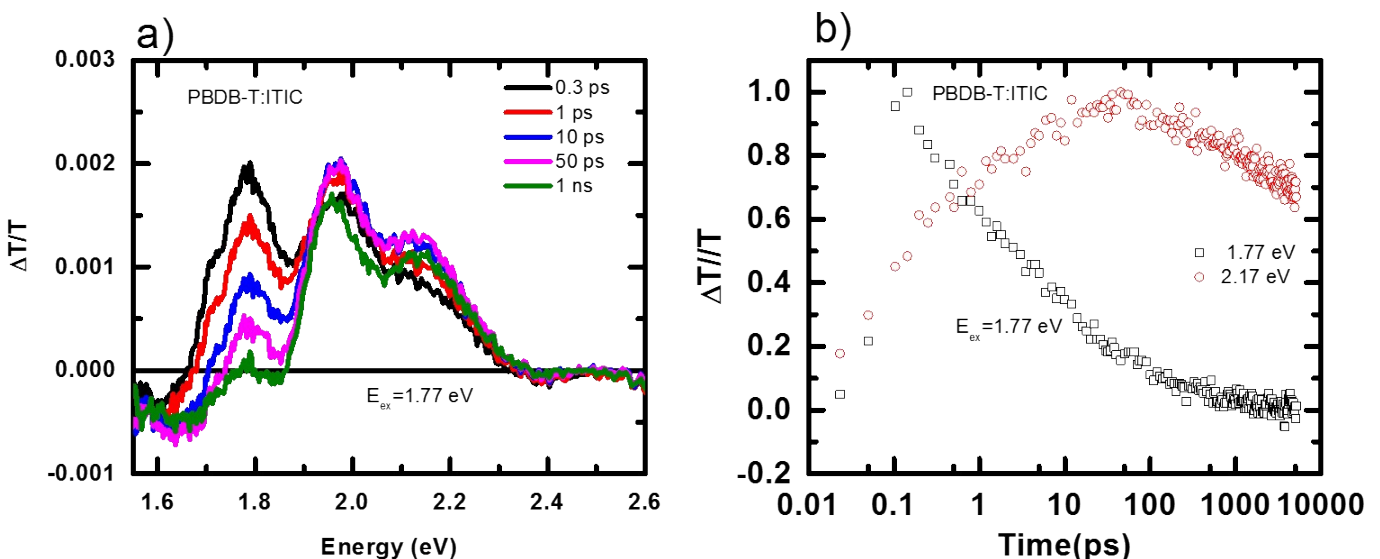


Figure S9: Visible range transient absorption spectra and transient absorption dynamics of PBDB-T:ITIC with 1.77 eV excitation.

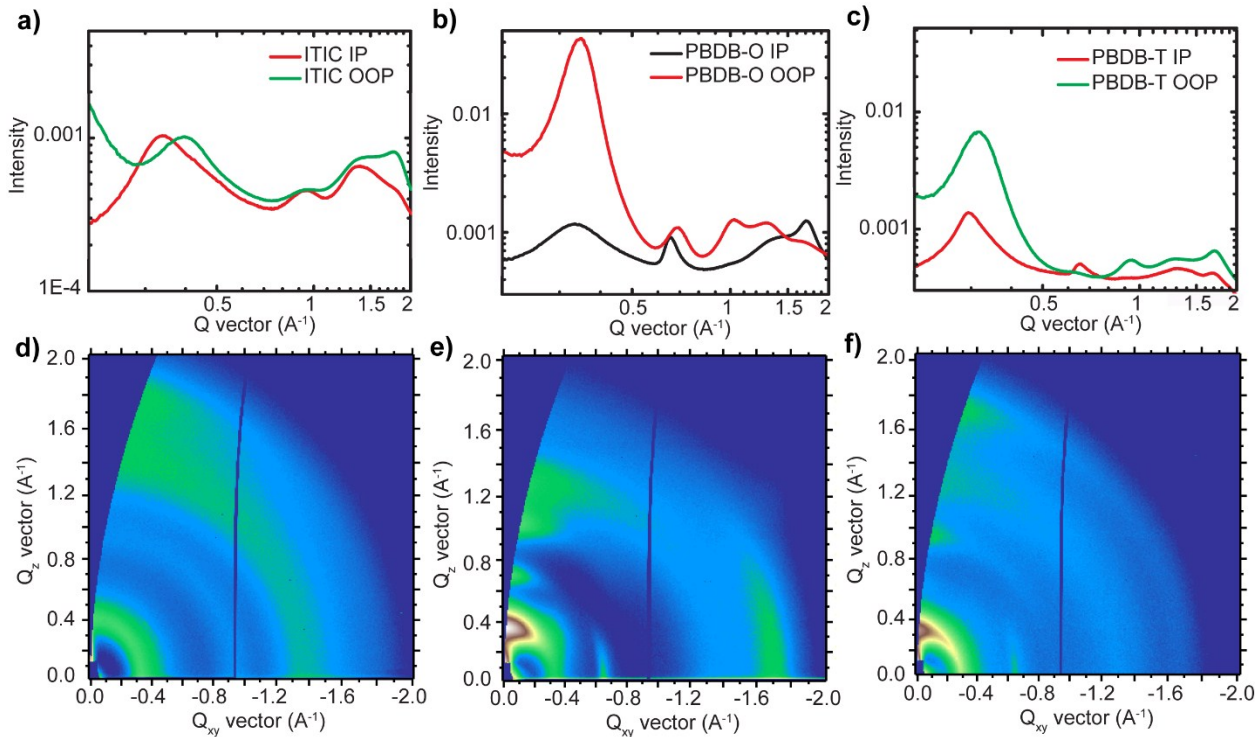


Figure S10. 1-D GIWAXS in-plane and out-of-plane linecuts for a) Neat ITIC, b) Neat PBDB-O, c) Neat PBDB-T. 2-D GIWAXS patterns at 0.15° for d) Neat ITIC, e) Neat PBDB-O and f) Neat PBDB-T.

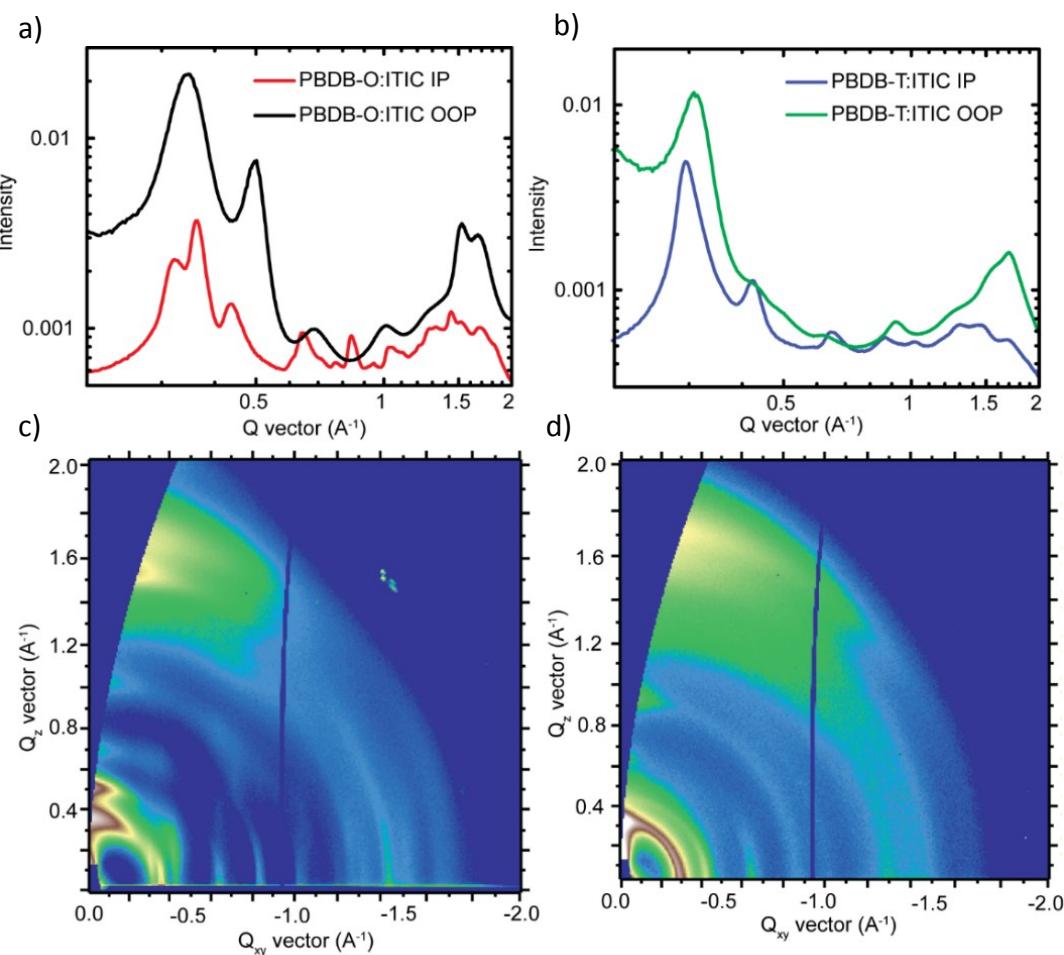


Figure S11. 1-D GIWAXS in-plane and out-of-plane linecuts for a) PBDB-O:ITIC, b) PBDB-T:ITIC. 2-D GIWAXS patterns at 0.12° (critical angle) for c) PBDB-O:ITIC, d) PBDB-T:ITIC.

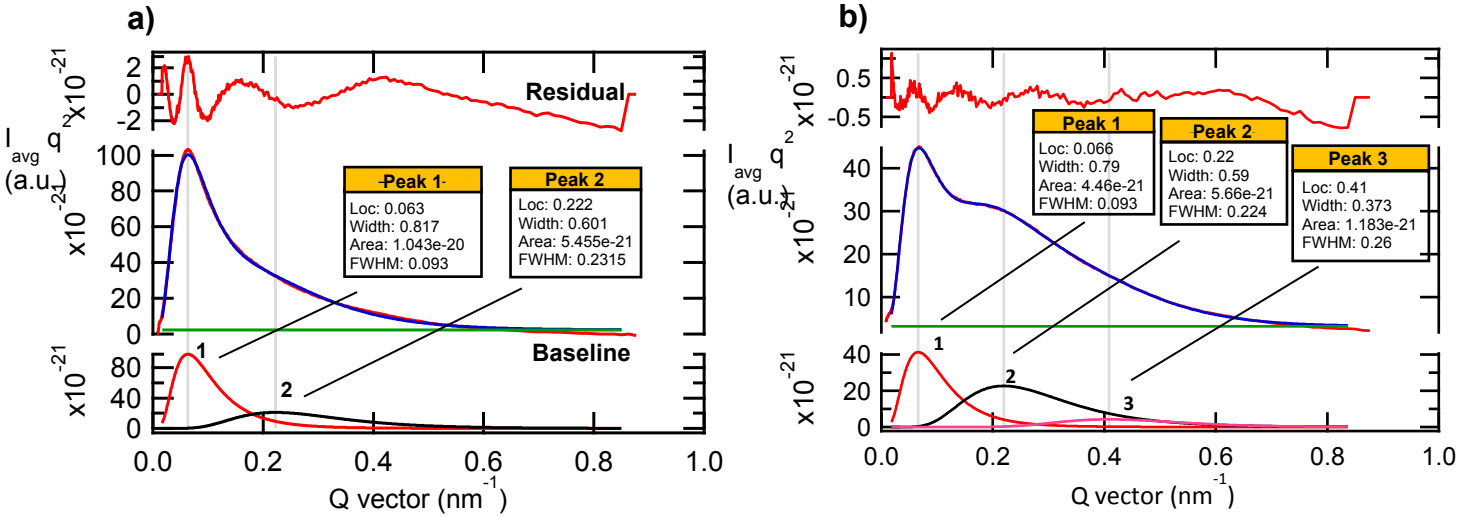


Figure S12. RSoXS profiles at 284.2 eV with Lognormal peak fitting and residual for a) PBDB-O:ITIC and b) PBDB-T:ITIC blend films. The location, width, area and FWHM for each of the peaks are provided using the Lognormal fits. Since there is no noticeable fluorescence in either of the blends at this energy, a constant line was assumed for the scattering background.